

Instability Analysis of Strike-Slip Fault Based on Cusp Catastrophe Model

Zaitie Chen^{1,*}, Wei Wang² and Dayang Li³

Abstract: The distribution of many active faults in western China is an important reason for the frequent earthquakes. With the rapid development of the western region, many major projects have been built there and the existence of active faults is bound to have an influence on the safety of the engineering structure. Therefore, it is of great significance to study the mechanism of fault slip instability for evaluating the geological stability of the region and for the site selection of major projects. In this paper, cusp catastrophe theory is used to establish a cusp catastrophe model with general softened form of strike-slip faults on the basis of strike-slip faults. In this model, the influence of the softening property of fault zone on fault instability is considered. Based on this model, the conditions of slip instability of strike-slip faults are derived and further the half-slip distance, far-field displacement and energy release equation of sliding-slip fault are revealed. The influences of the system stiffness ratio and the softening property of the fault zone on the half-wave displacement, the far-field displacement and the energy release are shown. Which lays a good foundation for further research on active fault-induced earthquake mechanism.

Keywords: Cusp catastrophe model, strike-slip fault, semi-dislocation, far field displacement.

1 Introduction

With the rapid development of the strategy for the great development of Western China, many major projects have been set up in the western region. Due to the geological structure and the plate movement, the western region has a lot of active faults due to the active geological movement, which is one of the important reasons for the earthquake. Therefore, studying the mechanism of fault slip instability is of great significance for the evaluation of the geological stability in the area and the location of major projects. The slip instability of the fault can be regarded as the limit instability of the system, that belongs to the extreme point instability, and which is a discontinuous state of the fault system [Yin (1984)].

Due to the complexity of the fault system, it is still difficult to seek accurate description

¹ Shazhou Institute of Technology, Zhangjiagang 215600, China.

² Yangzhou Vocational College, Yangzhou 225009, China.

³ Department of Engineering Mechanics, Hohai University, Nanjing 210098, China.

* Corresponding author: Zaitie Chen. Email: chenzaitie@qq.com.

of the mechanism of fault slip instability by using traditional mechanics methods. However, catastrophe theory does not need to consider its intrinsic mechanism because it can directly deal with the system discontinuity [Dou and Ghose (2006)], that provides a feasible method for studying the stick-slip instability of faults. Catastrophe theory is to study the state of the system with the continuous change of external control variables and the occurrence of discontinuous changes in mathematical theory. Catastrophe theory has been applied in engineering instability problems such as rock mass destruction [Chenglin, Pei, Huang et al. (2016); Xia, Liu, Chen et al. (2015); Pellet and Benoit (1999)], cavern and slope instability [Jeon, Kim, Seo et al. (2004); Chen and Wei (2003); Kirzhner and Rosenhouse (2000); Wang, Lam, Au et al. (2006)] and so on. In the aspect of fault instability, some scholars apply the catastrophe theory to study this problem. Yin [Yin (1984)] first proposed the cusp catastrophe model of fault instability and pointed out that the softening property of the fault is a necessary condition for system instability. On this basis, Yang et al. [Yang and Yin (1994)] took the compressive-torsional fault as the object, and deduced the cusp catastrophe form of the compressive-torsional fault instability by using the simplified constitutive relation; it is further pointed out that the intrinsic factors (stiffness ratio, softening property), the external factors (tectonic action and confining pressure) also have an important influence on the fault instability. Shi et al. [Shi, Luo, Peng et al. (1996)] use the cusp catastrophe theory to further analyze the influence of external forces on the fault slip instability, proposed the critical value of the external force when the fault slip instability. Pan et al. [Pan and Zhao (2012); Pan and Ai (2010)] analyzed the effect of the confining pressure, the maximum principal stress and the dip angle on the thrust fault instability by using the catastrophe mutation model. These studies have focused on the seismogenic mechanism of fault instability.

In addition, some scholars have explored the consequences of fault instabilities through various methods. Pelap et al. [Pelap, Kagho and Fogang (2016)] considered the dynamics of a modified 1D nonlinear spring-block model for earthquake studies to the strengths induced by the motion of the tectonic plates and the up flow of magma during volcanism; some scholars used numerical tests to study the generation of micro-cracks in the fault and the energy release factors [Tang, Tham, Wang et al. (2007); Jih and Sun (1990); Yan, Liu and Mai (2003); Jiang, Feng, Xiang et al. (2010); Weng, Huang, Taheri et al. (2017)], and scholars used model tests to study different materials and different types of faults. The consequences and factors of instability have yielded useful conclusions [He, Miao and Feng (2010); Song, Ma, Yang et al. (2011)]. Although it has become a consensus that the fault zone has the softening property as a necessary condition for the fault instability, the effect of faults with different softening properties on the system instability, and after instability the influence of faults with different softening properties on the faults, far-field displacements and energy release during system instability have not been studied systematically.

In order to deal with the above two problems, a general cusp catastrophe model is established in this paper, based on the horizontal strike-slip fault. This model introduced the parameter which considered different softening properties of the fault zone, and systematically studied the characteristics of fault softening; the relationship between the stiffness ratio of fault and surrounding rock system and the sliding instability of

strike-slip fault is analyzed. The influence of softening property and system stiffness ratio on the fault offset, far-field displacement and energy release in the event of fault instability is obtained.

2 Catastrophe theory

Rene Thom studies the discontinuities systematically by using the mathematical methods of topology and singularity theory, and the catastrophe theory is proposed for the first time. Catastrophe theory uses mathematical tools to describe the state of the system leap: given the system is in a stable parameter area, the variation of parameters can result in the change of system state if the parameters pass through certain locations [Thom (1994)]. Catastrophe theory proposes a series of mathematical models to explain the discontinuous processes of changes in nature and in social phenomena, and to describe the reason why various phenomena have suddenly jumped from one form to another radically different one. Such as the rock burst, the collapse of the geological, earthquakes, biological variation, market changes, business failures, economic crisis [Zhang, Shu, Zhang et al. (2015); Wen, Chen, Xiao et al. (2016); Guglielmi (2015); Hathout (2015); Zhao and Wang (1993); Ceniceros (2006); Scapens, Ryan and Fletcher (2010); Schenker-Wicki, Inauen and Olivares (2010)]. In general, Catastrophe theory contains seven elementary catastrophe models: fold catastrophe, cusp catastrophe, swallowtail mutation, butterfly mutation, hyperbolic umbilic point, elliptic umbilic and parabolic umbilic. Among them, the cusp catastrophe theory is widely used because of its simple form and convenient mathematical treatment [Golubitsky (2006)].

From Fig. 1, the point $P(x, p, q)$ of the system state are located at the upper and lower leaves of the equilibrium surface. Regardless of the path of p, q , the middle leaves are always unreachable. In most cases, the smoothing change of p, q always causes a smooth change of x (such as trajectory BB'). However, when the trajectory passes through the bifurcation set, the small change of p and q can cause the phase of the catastrophe: the point P will jump to another leaf, causing the state variable x catastrophe and as a result, the system will change from the critical equilibrium state to a stable equilibrium state. The cusp catastrophe model shows the discontinuity of the system properties.

The state of the system can be determined by the control variables p, q and a state variable x . In the three-dimensional state space composed of (x, p, q) , the standard form of its potential function is:

$$V = \frac{1}{4}x^4 + \frac{1}{2}px^2 + qx \quad (1)$$

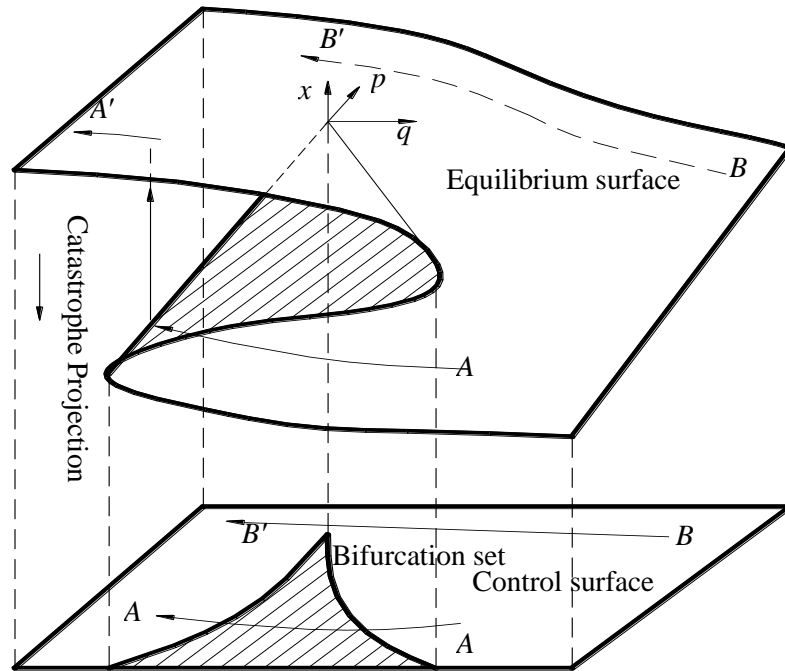


Figure 1: The equilibrium surface of the cusp catastrophe model and the bifurcation

Balance surface M (Fig. 1) is the set of all equilibrium points, the equilibrium point should meet:

$$V'(x) = x^3 + px + q = 0 \quad (2)$$

In the (x, p, q) space, it is a smooth curved surface with folds, which has the five characteristics of sudden jump, bimodal, hysteresis, divergence and reachability.

The mutation point or singular point satisfies both (2) and (3):

$$V'' = 3x^2 + p = 0 \quad (3)$$

Their projection on the control variable $p-q$ plane constitutes the bifurcation set B . Simultaneous Eqs. (2), (3) eliminate x to get the shape of a semi-cubic parabola set:

$$4p^3 + 27q^2 = 0 \quad (4)$$

Equilibrium surface Eq. (2) is a typical Cartan cubic equation, the discriminant of the root is $\Delta = 4p^3 + 27q^2$. When $\Delta > 0$, there is a real root and two complex roots. Therefore, there is only one equilibrium point for any (p, q) except for the bifurcation set, including half-space $p > 0$. $V'' > 0$, which is a stable equilibrium solution according to the stability theory of elastic system. When $\Delta = 0$, that is, there are 3 real roots when satisfying formula (4): if $x = p = q = 0$, there is a triple zero; if $4p^3 = -27q^2 \neq 0$ (left and right branch except for the cusp), two of the three real roots are the same, that is, there are two equilibrium points, one of which is stable equilibrium, and the other is the critical balance; when $\Delta < 0$, there are three different real roots with $V'' < 0$ in this region, so there

are three equilibrium points within the bifurcation set (shaded area in Fig. 1), two of which are stable balance, one is unstable balance.

3 Cusp catastrophe model for fault slip

3.1 General softening model of fault

Assume a horizontal strike of the fault and the uniform medium rock composed of the mechanical system, as shown in Fig. 2. The distance from the boundary of the far-field boundary to the edge of the fault zone is B , and the width of the fault zone is $2b$, and the coordinates (u, v, z) are established as shown. Set the far field displacement to u_∞ , the displacement of the fault u_f , the displacement of the surrounding rock u_s , obtained from Fig. 2:

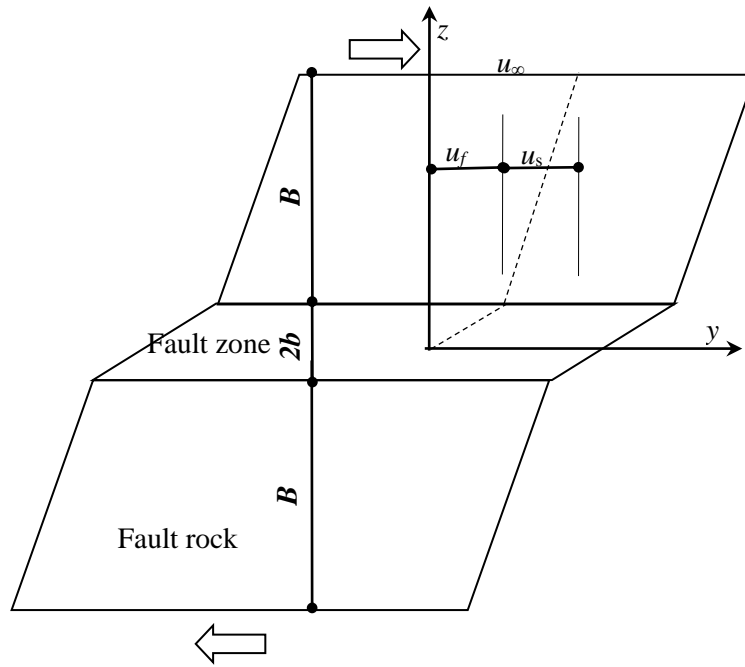


Figure 2: Model of fault-surrounding rock

$$u_\infty = u_s + u_f \tag{5}$$

The surrounding rock is isotropic elastic medium, which satisfies Hooke's law:

$$\tau_s = G_s \gamma_s \tag{6}$$

where, τ_s is the surrounding rock shear stress; G_s is rock shear stiffness; γ_s is the rock shear strain. For the sake of convenience, it is represented as the form of shear displacement u_s : (R_s shear force)

$$R_s = K_s u_s \tag{7}$$

In Eq. (7), $K_s = G_s A / B$, A is the cross section area of the fault surrounding rock system.

Based on the inhomogeneity of fault surface strength, the macro fracture process of

fracture surface is regarded as the accumulation process of local microelement of fault. It is assumed that the local microelement intensity of fault follows Weibull probability distribution [Li and Yin (2009)]. The stress and strain relation of the fault zone is taken as a negative exponential form [Stuart (1979)]:

$$\tau_f = G_f \gamma_f \cdot e^{-\left(\frac{\gamma_f}{\gamma_0}\right)^m} \quad (8)$$

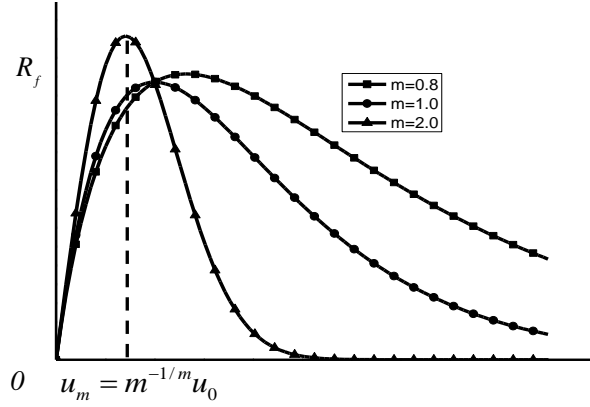
In Eq. (8), The τ_f is shear stress; G_f is fault initial shear stiffness; γ_f is shear strain. The shear displacement u_f of the fault zone and the strain γ_f satisfy the geometric equation:

$$\gamma_f = \frac{u_f}{b} \quad (9)$$

Letting $K_f = \frac{G_f A}{b}$, the relationship between the shear force- shear displacement of the fault zone becomes:

$$R_f = K_f u_f \cdot e^{-\left(\frac{u_f}{u_0}\right)^m} \quad (10)$$

The function graph is shown in Fig. 3. Where u_0 is a constant; m is the shape parameter, which is related to the mechanical properties of the fault medium. In previous studies, more attention was focused on the application of catastrophe theory to fault instability, and the convenience of establishing a mutation model often makes $m=1$ [Yin (1984, 1988)]. This treatment ignores the influence of the properties of fault media on fault instability and the energy release, offset and far-field displacements of the fault after fault failure. Therefore, in order to discuss the effect of the fault zone on the fault instability, based on the form of fault softening model, a cusp catastrophe model considering the properties of fault zone is established in this paper.


Figure 3: Shear stress~shear displacement

3.2 A cusp catastrophe model of moving fault in moving fault

While $R_f'' = 0$, the catastrophe point corresponding to the curve is:

$$u^* = m \sqrt{\frac{m+1}{m}} \cdot u_0 \quad (11)$$

For the sake of convenience, the fault displacement takes $u_f = u$. Regardless of the influence of gravity, the total potential energy of the fault surrounding rock system is

$$V = \int_u^{u_\infty} R_s \cdot du_s + \int_0^u R_f \cdot du = \int_u^{u_\infty} K_s u_s du_s + \int_0^u K_f u \cdot e^{-\left(\frac{u}{u_0}\right)^m} du \quad (12)$$

Deriving the equation of the formula (12), the equation of the equilibrium surface is obtained:

$$V' = K_f u \cdot e^{-\left(\frac{u}{u_0}\right)^m} + K_s (u_\infty - u) = 0 \quad (13)$$

Eq. (13) is taken into the power series form at the inflection point $u = u^*$ of the $R_f - u$ curve. By intercepting the power series at the third order, the equation becomes:

$$\begin{aligned} & K_f \cdot u^* \cdot e^{-\left(\frac{u^*}{u_0}\right)^m} + K_s \cdot (u_\infty - u^*) + \left(K_f \cdot e^{-\left(\frac{u^*}{u_0}\right)^m} \cdot \left(1 - m \left(\frac{u^*}{u_0} \right)^m \right) + K_s \right) (u - u^*) - \\ & \frac{1}{2} m \cdot K_f \cdot \frac{u^{*m-1}}{u_0^m} \cdot e^{-\left(\frac{u^*}{u_0}\right)^m} \cdot \left(m + 1 - m \cdot \left(\frac{u^*}{u_0} \right)^m \right) \cdot (u - u^*)^2 - \frac{1}{6} m \cdot K_f \cdot e^{-\left(\frac{u^*}{u_0}\right)^m} \cdot \\ & \left(\left((m^2 - 1) \cdot \frac{u^{*m-2}}{u_0^m} - 3m^2 \cdot \frac{u^{*2m-2}}{u_0^{2m}} + m^2 \cdot \frac{u^{*3m-2}}{u_0^{3m}} \right) \right) \cdot (u - u^*)^3 = 0 \end{aligned} \quad (14)$$

Letting $u^* = \sqrt[m]{\frac{m+1}{m}} \cdot u_0$, the Eq. (15) is obtained:

$$\left(\frac{u-u^*}{u^*}\right)^3 + \frac{6}{m \cdot (m+1)^2} \cdot \left(\frac{K_s}{K_f \cdot e^{-\frac{m+1}{m}}} - m\right) \left(\frac{u-u^*}{u^*}\right) + \frac{6}{m \cdot (m+1)^2} \cdot \left(1 - \frac{K_s}{K_f \cdot e^{-\frac{m+1}{m}}} \left(\frac{u_\infty - u^*}{u^*}\right)\right) = 0 \quad (15)$$

Eq. (15) is in the standard form of the cusp catastrophe model for fault slip. By considering $K = \frac{K_s}{K_f m e^{-\frac{m+1}{m}}} = \frac{K_s}{K_f}$, $\xi = \frac{u_\infty - u^*}{u^*}$, the (p, q, x) coordinate system

becomes:

$$x = \frac{u - u^*}{u^*} \quad (16)$$

$$p = \frac{6}{(m+1)^2} \cdot (K - 1) \quad (17)$$

$$q = \frac{6}{(m+1)^2} \cdot \left(\frac{1}{m} - K\xi\right) \quad (18)$$

The physical meaning of the above formula is: K is: the ratio of the stiffness of the surrounding rock to the slope of the softening constitutive curve at the inflection point; ξ , called the full displacement parameter, is the dimensionless parameter associated with the far field displacement .

When $4p^3 = -27q^2 \neq 0$ (left and right branches except the cusp), the mutation point corresponding to the critical equilibrium state is

$$x_1 = \sqrt[3]{q/2} = \pm \sqrt{-\frac{p}{3}} = \pm \frac{1}{m+1} \sqrt{2(1-K)} \quad (19)$$

The solution corresponding to the steady equilibrium state is:

$$x_2 = \sqrt[3]{-4q} = -2x_1 \quad (20)$$

The displacement corresponding to the mutation point x_l is:

$$u_k = u^* (1 + x_1) \quad (21)$$

In Eq. (19), the X_l should take the negative value because the change of the displacement is, in general, larger than the change of the load. That is to say should be taken (19) the minus sign (corresponding to $q < 0$), which should be considered when x

left across the bifurcation set mutation situation.

3.3 The condition of active fault sliding instability

The point of the equilibrium surface changes within the control plane (p, q), and the number and stability of the system will not change as long as it does not cross the bifurcation set. Once the bifurcation set is crossed, the system properties will mutate. Only when $p \leq 0$, the bifurcation set will exist, so $p \leq 0$ is a necessary condition for system instability. Substituting the inequality in to Eq. (17) leads to:

$$K = \frac{K_s}{K_f m e^{-\frac{m+1}{m}}} = \frac{K_s \cdot e \cdot e^{1/m}}{m K_f} \leq 1 \tag{22}$$

That is, the necessary condition of system instability is that the ratio of the stiffness of surrounding rock and fault softening inflection point is less than 1. According to Eq. (22), it can be concluded that larger m value, greater initial stiffness of the fault zone, and greater brittleness of the fault zone, make the formula (22) easier to be satisfied, increasing the probabilities of instability of the fault system.

In order to determine the value of the far field displacement parameter, ξ , at the time of crossing the bifurcation set, formula (17), (18) are substituted into Eq. (4):

$$\xi = \frac{1}{Km} \cdot \left[1 \pm \frac{2\sqrt{2m}}{3(m+1)} \cdot (1-K)^{3/2} \right] \tag{23}$$

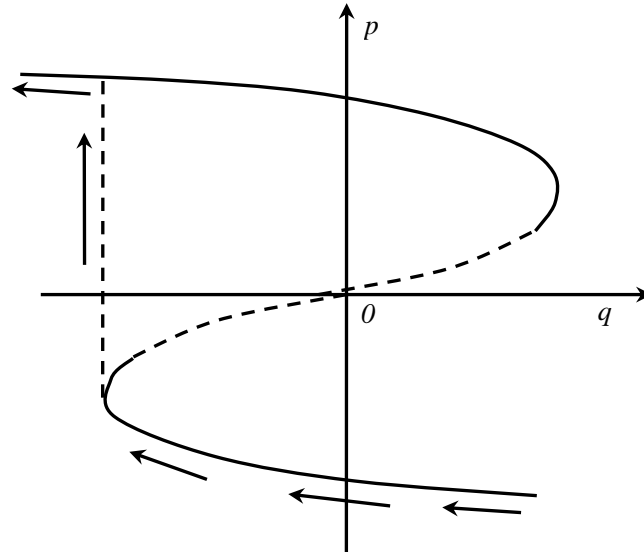


Figure 4: Catastrophic state variable in burrification

Formula (18) implied that for a smaller zeta value, the right branch is located in the bifurcation set ($q > 0$). As shown in Fig. 5, when increasing of zeta, q decreased gradually. Only when $q < 0$, and across the left bifurcation set, the state variable x can jump. Thus, the plus in Eq. (23) should be accepted.

4 Effect of fault softening coefficient on fault half distortion, far field displacement and energy release

Far-field displacements, misalignment distances (faults) and energy release after fault failure are important parameters to evaluate fault activity. They can reflect the degree of damage to major projects caused by slip and instability of active faults. Therefore, it is necessary to study the fault dislocation, far-field displacement and energy release caused by fault movement. Because of utilization of the symmetrical form of the fault model, the semi-dislocation is employed to represent the fault-zone offset.

In the cusp catastrophe model, state variables mutate when crossing a bifurcation set. The magnitude of the abrupt change of the left branch system state variable x is:

$$\Delta x = x_2 - x_1 = \frac{3}{m+1} \sqrt{2(1-K)} \quad (24)$$

The semi-dislocation before and after the system instability of the fault interval is:

$$\Delta u = u_2 - u_1 = \Delta x \cdot u^* = \frac{3\sqrt{2}}{m+1} \sqrt{\frac{m+1}{m}} \sqrt{1-K} \cdot u_0 \quad (25)$$

The far field displacement at the time of system mutation is:

$$u_\infty = (1 + \xi) \cdot u_f^* = \left[1 + \frac{1}{K} \cdot \left(\frac{1}{m} + \frac{2\sqrt{2}}{3(m+1)} \cdot (1-K)^{3/2} \right) \right] \cdot \left(\frac{m+1}{m} \right)^{1/m} \cdot u_0 \quad (26)$$

The energy release during the process of instability can be estimated by the energy difference before and after the system mutation. The energy expression, corresponding to the sharp point of the start, is cut to four terms, and the non-dimensional potential energy can be obtained:

$$V = \frac{1}{24} \cdot m(m+1)^2 \cdot \left(\frac{m+1}{m} \right)^{2/m} \cdot e^{-\frac{m+1}{m}} \cdot K_f \cdot u_0^2 \cdot [x^4 + 2px^2 + 4qx + c] \quad (27)$$

where,

$$c = \frac{12\xi}{(m+1)^2} + \frac{24e^{\frac{m+1}{m}}}{m(m+1)^2} \cdot \frac{1}{(u_f^*)^2} \cdot \int_0^{u_f^*} u \cdot e^{-\left(\frac{u}{u_0}\right)^m} du \quad (28)$$

The formula (27) is divided by $K_f \cdot u_0^2$, leading to the dimensionless quantity:

$$U = \frac{V}{K_f \cdot u_0^2} \quad (29)$$

The dimensionless expression of the energy release before and after the instability of the system is as follows:

$$\begin{aligned} \Delta U &= \frac{1}{24} \cdot m(m+1)^2 \cdot \left(\frac{m+1}{m}\right)^{2/m} \cdot e^{-\frac{m+1}{m}} \cdot [x_1^4 - x_2^4 + 2p(x_1^2 - x_2^2) + 4q(x_1 - x_2)] \\ &= \frac{7m}{2(m+1)^2} \cdot \left(\frac{m+1}{m}\right)^{2/m} \cdot e^{-\frac{m+1}{m}} \cdot (1-K)^2 \end{aligned} \quad (30)$$

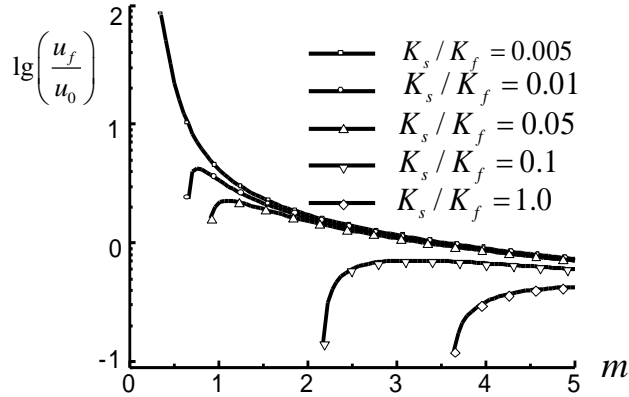


Figure 5: While fault slipping: Half dislocation ~m

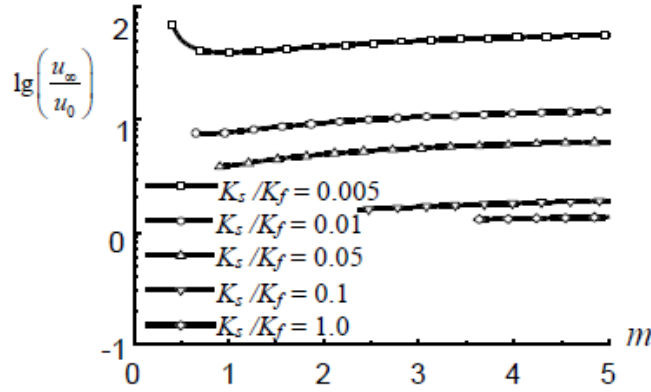


Figure 6: While fault slipping: Remote displacement ~m

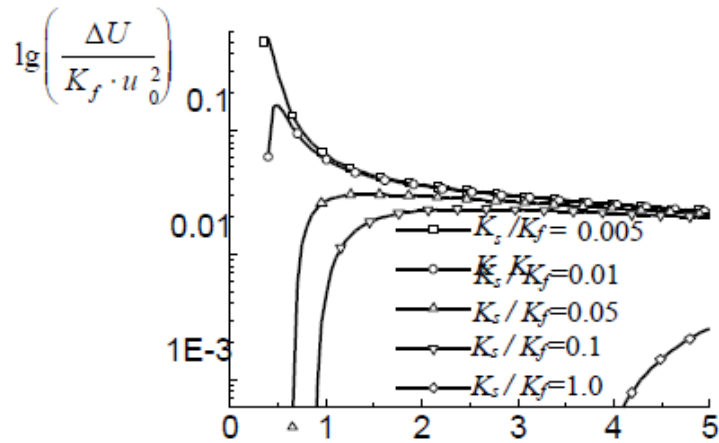


Figure 7: While fault slipping: Dimensionless release energy~ m

Fig. 5 shows the influence of the stiffness ratio and the softening coefficient on the half-staggered distance. It can be seen from the figure that when the system stiffness is relatively small, the fault moment generated when the fault is unstable is larger, and the error distance gradually decreases with the increase of m , and reaches a stable value eventually. When the stiffness is relatively large, with the increase of m , the error gradually increases, and finally reaches a stable value.

In the cases of different stiffness ratios, the relationship between far-field displacement and m value is shown in Fig. 6. When the stiffness is relatively small, the far-field displacement generated when the fault is unstable is large. When the stiffness is relatively large, the far-field displacement generated when the fault is unstable is small. And when the stiffness ratio is consistent, far-field displacement has little to do with the value of m . This indicates that the relation between far-field displacement and m is weak, and the far-field displacement depends mainly on the system stiffness ratio.

In the cases of different stiffness ratios, the relationship between the dimensionless value of the system energy release and the value of m is shown in Fig. 7. It can be seen from the figure that when the stiffness is relatively small, the energy released during the failure of the fault is large. With the increase of the m value, the energy release is significantly reduced and reaches a stable value. When the stiffness is relatively large, the energy release during the instability is much smaller for a fixed m . With the increase the value of m , the energy release gradually increases and finally reaches a stable value.

5 Conclusion

Taking the horizontal strike-slip fault model as an example, based on the cusp catastrophe theory model, the instability characteristics of strike-slip faults with general softening form constitutive relations are analyzed, and the critical conditions of strike-slip faults are deduced. Effect of m value of softening curve (initial stiffness of fault zone) on half-stagger due to unsteady movement of active fault, far-field displacement in case of instability and energy release are investigated. The results show:

(1) Larger fault softening coefficient, and brittleness, make the higher probability of instability of the fault-surrounding rock system. In addition, bigger difference between the fault and the surrounding rock stiffness can lead to a more destabilized fault. Such faults can easily induce earthquakes. When the system stiffness ratio approaches 1, the system is not prone to instability;

(2) The half-fault of fault zone, the far-field displacement and energy the release during instability, are mainly related to the difference between fault and surrounding rock stiffness. For faults surrounded by rocks with great difference in stiffness, the instability is much easier to take place, which can induce earthquakes and result in great damage. For such faults, monitoring needs to be strengthened. In addition, since the softening property of the faults becomes more prominent and the half-stagger and energy release gradually decrease, such faults can easily become seismic. However, the small energy release shows that the sustained, smaller fault rupture, to some extent, can reduce the energy accumulation, cutting down the possibility of occurrences of large earthquakes.

Although the cusp catastrophe model is not capable of reflecting the complex mechanics environment of actual faults because of its simple form, the research results of this paper can lay a foundation for the further study of active fault-induced earthquakes.

Reference

Ceniceros, R. (2006): Catastrophe model changes tighten market for storm risks. (Spotlight: Catastrophe Risk Management). *Business Insurance*.

Chen, H.; Wei, Y. (2003): The formulation of fault engineering effect in whole. *Geotechnical Engineering Technique*, pp. 249-252.

Chenglin, M.; Pei, X.; Huang, R.; Pei, Z.; Lu, J. (2016): Study on instability criterion of layered rock mass failure based on cusp mutation theory. *Safety in Coal Mines*, vol. 47, no. 11, pp. 36-40.

Dou, W.; Ghose, S. (2006): A dynamic nonlinear model of online retail competition using cusp catastrophe theory. *Journal of Business Research*, vol. 59, no. 7, pp. 838-848.

Golubitsky, M. (2006): An introduction to catastrophe theory and its applications. *Siam Review*, vol. 20, no. 2, pp. 65-100.

Guglielmi, A. V. (2015): Foreshocks and aftershocks of strong earthquakes in the light of catastrophe theory. *Physics-Uspokhi*, vol. 58, no. 4, pp. 415-429.

Hathout, I. (2015): On the applications of catastrophe theory in engineering mechanics. *Engineering Mechanics in Civil Engineering*.

He, M.; Miao, J.; Feng, J. (2010): Rock burst process of limestone and its acoustic emission characteristics under true-triaxial unloading conditions. *International Journal of Rock Mechanics and Mining Sciences*, vol. 47, no. 2, pp. 286-298.

Jeon, S.; Kim, J.; Seo, Y.; Hong, C. (2004): Effect of a fault and weak plane on the stability of a tunnel in rock-a scaled model test and numerical analysis. *International Journal of Rock Mechanics & Mining Sciences*, vol. 41, no. 3, pp. 658-663.

Jiang, Q.; Feng, X. T.; Xiang, T. B. ; Su, G. (2010): Rockburst characteristics and numerical simulation based on a new energy index: A case study of a tunnel at 2,500 m depth. *Bulletin of Engineering Geology and the Environment*, vol. 69, no. 3, pp. 381-388.

Jih, C.; Sun, C. (1990): Evaluation of a finite element based crack-closure method for calculating static and dynamic strain energy release rates. *Engineering Fracture Mechanics*, vol. 37, no. 2, pp. 313-322.

Kirzhner, F.; Rosenhouse, G. (2000): Numerical analysis of tunnel dynamic response to earth motions. *Tunnelling & Underground Space Technology Incorporating Trenchless Technology Research*, vol. 15, no. 3, pp. 249-258.

Li, E. P.; Yin, Y. Q. (2009): A simply model for earthquake instability. *Earthquake Research in China*, vol. 24, no. 2, pp. 179-189.

Pan, Y.; Ai, W. L. (2010): Fold catastrophe model of strike-slip fault earthquake. *Applied Mathematics and Mechanics*, vol. 31, no. 3, pp. 349-362.

Pan, Y.; Zhao, Z. (2012): Analysis of main shock of thrust fault earthquake by catastrophe theory. *Applied Mathematics and Mechanics*, vol. 33, no. 7, pp. 845-864.

Pelap, F.; Kagho, L.; Fogang, C. (2016): Chaotic behavior of earthquakes induced by a nonlinear magma up flow. *Chaos, Solitons & Fractals*, vol. 87, pp. 71-83.

Pellet, F.; Benoit, O. (1999): 3-D numerical simulation of the behaviour of underground structures crossing faulted zone. *9th ISRM Congress*, pp. 213-218.

Scapens, R. W.; Ryan, R. J.; Fletcher, L. (2010): Explaining corporate failure: A catastrophe theory approach: Explaining corporate failure. *Journal of Business Finance & Accounting*, vol. 8, no. 1, pp. 1-26.

Schenker-Wicki, A.; Inauen, M.; Olivares, M. (2010): Unmastered risks: from crisis to catastrophe: An economic and management insight. *Journal of Business Research*, vol. 63, no. 4, pp. 337-346.

Shi, Z.; Luo, Z. ; Peng, D. ; He, Z. (1996): Application of catastrophe theory to the analyses of mechanism of faulting movement. *Journal of Xian Engineering University*, vol. 18, no. 1, pp. 50-55.

Song, Y.; Ma, S.; Yang, X.; Jiang, Y. (2011): Experimental investigation on instability transient process of fault rockburst. *Chinese Journal of Rock Mechanics and Engineering*, vol. 30, no. 4, pp. 812-817.

Stuart, W. D. (1979): Strain-softening instability model for the san fernando earthquake. *Science*, vol. 203, no. 4383, pp. 907.

Tang, C.; Tham, L.; Wang, S.; Liu, H.; Li, W. (2007): A numerical study of the influence of heterogeneity on the strength characterization of rock under uniaxial tension. *Mechanics of Materials*, vol. 39, no. 4, pp. 326-339.

Thom, R. (1994): *Structural stability and morphogenesis*. Westview Press.

Wang, S.; Lam, K.; Au, S.; Tang, C.; Zhu, W. et al. (2006): Analytical and numerical study on the pillar rockbursts mechanism. *Rock Mechanics & Rock Engineering*, vol. 39, no. 5, pp. 445-467.

Wen, C.; Chen, Y.; Xiao, H. ; Bai, Y.; Su, W. (2016): Evaluation of karst collapse

risks based on catastrophe progression method. *China Sciencepaper*, vol. 11, no. 13, pp. 1539-1543.

Weng, L.; Huang, L.; Taheri, A. ; Li, X. (2017): Rockburst characteristics and numerical simulation based on a strain energy density index: A case study of a roadway in Linglong gold mine, China. *Tunnelling and Underground Space Technology*, vol. 69, pp. 223-232.

Xia, K.; Liu, X.; Chen, C. ; Song, Y; Ou, Z. et al. (2015): Analysis of mechanism of bedding rock slope instability with catastrophe theory. *Yantu Lixue/rock & Soil Mechanics*, vol. 36, no. 2, pp. 477-486.

Yan, W. ; Liu, H.; Mai, Y. (2003): Numerical study on the mode I delamination toughness of z-pinned laminates. *Composites Science and Technology*, vol. 63, no. 10, pp. 1481-1493.

Yang, X. X.; Yin, Y. Q. (1994): Cusp type catastrophe analysis of the earthquake process of compression torsion fault. *China Science (B Series Chemical Life Science Geology)*, pp. 656-663.

Yin, Y. Q. (1988): A cusp type catastrophic model of fault earthquake. *Chinese Journal of Geophysics*, pp. 658-663.

Yin, Y.; Hong, Z. (1984): The softening behaviour of fault zone medium and an instability model of earthquakes. *Acta Seismologica Sinica*, pp. 135-145.

Zhang, J.; Shu, J.; Zhang, H.; Ren, X.; Qi, J. (2015): Study on rock mass stability criterion based on catastrophe theory. *Mathematical Problems in Engineering*, vol. 2015, no. 2015.

Zhao, H. A.; Wang, S. (1993): Catastrophe theory and application of some main pest in agriculture. *Acta Agriculturae Boreali-occidentalis Sinica*, pp. 48-52.